



# Balkh International Journal of Natural Science

ISSN – P 0000 -0000 E: 0000- 0000

Vol. 1 NO.1 2025

URL: <https://bjns.ba.edu.af/index.php/bjns>

## Investigation of Structural, Electronic, and Magnetic Properties of Aluminum nitride Monolayer Doped with Rb and Cs

1. Bashir Ahmad Niazi<sup>1</sup>

Senior Teaching Assistant, Faculty of Science, Balkh University

2. Sayed Emaduddin Mansor

Teaching Assistant, Faculty of Education, Takhar University

**Received: 26/6/2025      Accepted: 31/10/2025      Published: 20/12/2025**

### Abstract

Spintronics is the study of electron spin in electronics, fundamentally different from conventional charge-based electronics. In it, in addition to the charge of the electron, spin is also used as an additional degree of freedom. This means that a larger amount of data can be stored or transmitted. This research, conducted in 2020 in a laboratory at Kharazmi University in Tehran, examines the spintronic applications of a single layer of aluminum nitride (AlN) doped with rubidium (Rb) and cesium (Cs). Today, aluminum nitride (AlN) has gained attention as a viable material for spintronic applications due to its suitable electrical and thermal properties. Doping this material with Rb and Cs can lead to changes in its electrical and magnetic properties, thereby providing new capabilities in the fields of magnetic memory, sensors, and spintronic transistors. Initially, two-dimensional AlN monolayers were simulated, and in the next phase, a doped layer with rubidium and cesium was created at a concentration of 6.25 percent and examined. Using this method, the structural, electrical, and

---

<sup>1</sup>. Email: [bashirahmadniazi2020@gmail.com](mailto:bashirahmadniazi2020@gmail.com)

magnetic properties of the doped AlN layers were obtained, along with the effects of various concentrations of Rb and Cs on their spin behavior.

The results indicate that this combination could enhance the performance of spintronic devices and contribute to the development of new technologies, particularly in the fabrication of high-speed non-volatile magnetic memories (permanent memories).

**Keywords:** Aluminum Nitride, Cesium, Doping, Rubidium and Spintronics

## 1. Introduction:

In the coming decades, rapid advancements in information and communication technologies have transformed information production and the scale of social networks. The persistent demand for acquiring and storing information has led to the development of high-performance computers and mobile devices, resulting in the access to and storage of massive data (Fong et al, 2012). Nanomagnetism and spintronics represent a rapidly expanding and increasingly important research field, with many of its applications already available in the market, and many others expected to enter the market in the near future (Zutic et al, 2006). This field emerged in the mid-1980s with the discovery of the giant magnetoresistance (GMR) effect, which marked the origin of spintronics (Li & Yang, 2016), which involves the use of the electron spin degree of freedom for transmitting, storing, or reading information, is of great significance, and currently, extensive research is being conducted on various aspects of this technology (Žutić et al, 2004). Published articles from 2009 to 2018 related to spintronics show that the amount of research in this field has steadily increased over these years (Paquin et al, 2015). In recent years, two-dimensional (2D) materials have received extensive attention because of their fascinating optical, mechanical, electronic, and magnetic properties and potential for multifunctional applications (Cui et al, 2018).

In this article, we aim to investigate the possibility of half-metallic behavior in some two-dimensional materials using the (DFT) density functional theory (Cui et al, 2018). Following the discovery of graphene, research on two-dimensional materials has intensified significantly, and some of these materials, due to their exceptional properties and atomic-scale thin structures, have been recognized as potential candidates for

spintronic applications. However, to use some of these materials in spintronics, modifications are required in other words; these materials need to be engineered (Xia et al, 2012). One of the methods for such modification is doping of the two-dimensional material.

Specifically, in this work, we aim to examine the effect of doping with rubidium and cesium atoms on the electronic and magnetic properties of AlN monolayers. For this purpose, we will utilize the density functional theory. The structure of this article is such that we will first briefly discuss spintronic, half-metals, and the applications of two-dimensional materials in spintronic technologies (Zhang & Hou, 2024). Finally, we will analyze the electronic and magnetic properties of AlN monolayers doped with rubidium and cesium. Most existing two-dimensional materials are non-magnetic semiconductors and thus are not directly applicable in spintronic. However, by adding different dopants, the properties of these materials can be effectively modified for spintronic applications (Han et al, 2017).

Group III nitrides such as boron nitride (BN), aluminum nitride (AlN), and gallium nitride (GaN) are among the compounds that exhibit diverse electronic, magnetic, and optical properties in both two-dimensional and three-dimensional forms (Bhatti et al, 2017). AlN was first synthesized in 1877, but it was not until 1980 that its significant potential for microelectronic applications was recognized, after which it entered the market as a valuable commercial material. Due to its high thermal conductivity and electrical insulation, AlN is used in microelectronic industries. Other applications include its use in military and aerospace industries, as well as in the ceramics industry for producing high-melting-point ceramics and refractory bricks. Therefore, research on these materials and their doping can have numerous applications (Chen et al, 2016).

One of the important goals and challenges in nano-spintronic devices may be the generation of spin-polarized currents. It seems that the use of semimetals is among the reliable methods for producing spin-polarized currents. These materials exhibit different electronic behaviors for spin-up and spin-down states, such that one spin channel shows metallic behavior while the other behaves like a semiconductor (Dean et al, 2010).

## 2. Materials and Methods

The results of the investigations show that the stable structure of monolayer aluminum nitride (AlN) is free of buckling (Ghasemzadeh & Kanjouri, 2018). Figure 1 illustrates the stable crystal structure of two-dimensional AlN monolayers, which was simulate using Win2k. As mentioned, a  $4\times 4$  supercell was use for the calculations. In fact, this structure is of the honeycomb lattice type, and from the crystallographic point of view, its unit cell is a simple hexagonal lattice with a two-atom basis. The lattice constant of this structure in the stable state is  $3.10\text{ \AA}$  (Dean et al, 2010).

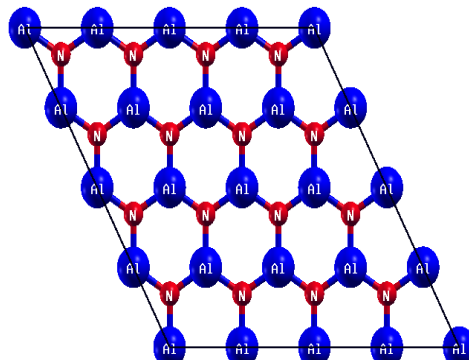


Figure1:  $4\times 4$  supercell of two-dimensional AlN monolayer using the WINN2k simulation package.

To investigate the electronic properties, the density of states (DOS) plot is shown in Figure 2. In this plot, positive values correspond to the spin-up DOS and negative values correspond to the spin-down DOS. As observed, there is complete symmetry between the spin-up and spin-down states, indicating that the monolayer is non-magnetic in its pristine (undoped) state (Wolf et al, 2006). Additionally, the Fermi level lies within the band gap; hence, this sample behaves as a semiconductor. The magnetic moment of the compound is also, as expected; zero (Bai et al, 2015).

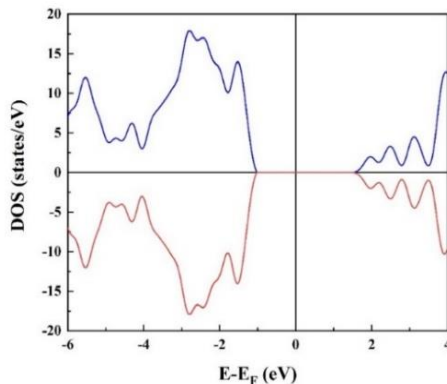


Figure 2: Density of states (DOS) plot of two-dimensional AlN monolayers. Positive values correspond to the DOS of spin-up electrons, and negative values correspond to the DOS of spin-down electrons. Using DFT calculations within the Quantum ESOERSSO simulation package.

Now, we proceed to simulate the two-dimensional AlN monolayer doped with Rb and Cs elements. Two supercells were constructe for this purpose, similar to Figure 1, with the difference that in each, one aluminum atom is substitute once by a rubidium atom and once by a cesium atom. Figure 3 shows these two supercells. To find the stable structures of the doped compounds, full atomic relaxation was performe in all three directions: x, y, and z. Figure 4 shows these supercells after relaxation (Gallagher & Parkin, 2006).The largest changes in atomic coordinates occur around the impurity atom; however, from the figures, it appears that atoms at the supercell boundaries have also undergone significant changes. In reality, this is not the case, and the changes at the boundaries are minimal. The apparent changes occur because atoms have moved into adjacent cells. To demonstrate this, Figures 5 and 6 respectively show the arrangement of several supercells side by side for the rubidium- and cesium-doped samples, clearly indicating that the greatest changes in atomic coordinates are around the impurity atom.

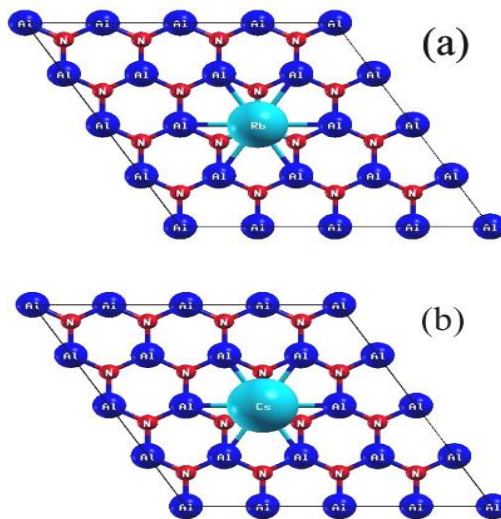


Figure 3: Doped supercells with (a) rubidium, (b) cesium before relaxation using the WINN2k simulation package.

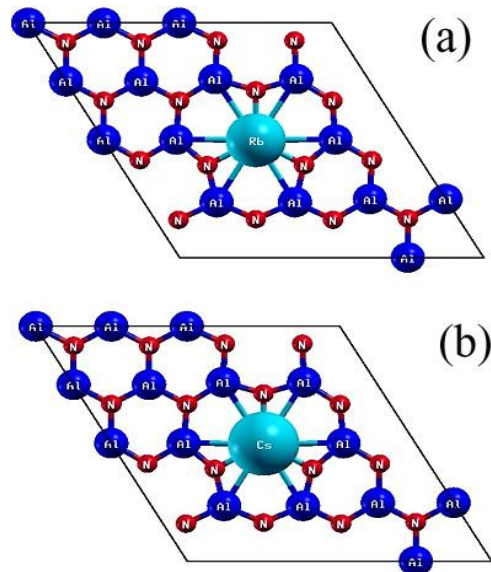


Figure 4: Doped supercells with (a) rubidium, (b) cesium after relaxation  
Using the WINN2k simulation package.

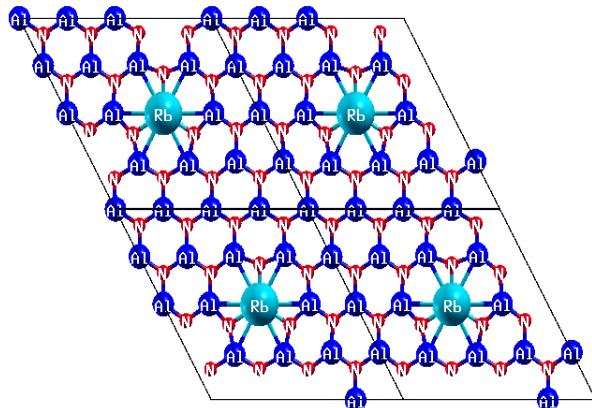


Figure 5: Arrangement of several supercells side by side for the rubidium-doped sample using the WINN2k simulation package.

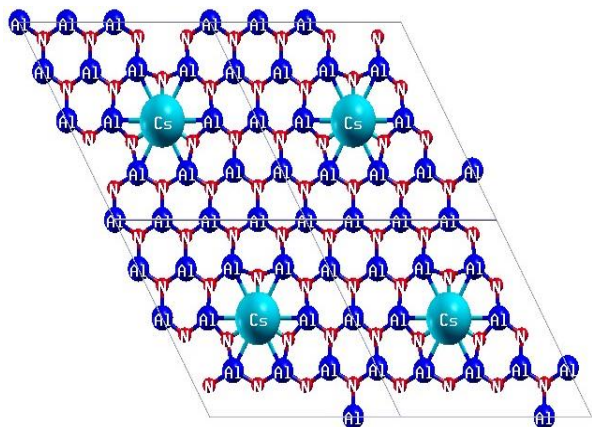


Figure 6:  
Arrangement of several supercells side by side for the cesium-doped sample using the WINN2k simulation package.

### 3. Results and Discussion

The analysis reveals that the incorporation of impurity atoms does not induce buckling in the two-dimensional AlN monolayer; structural distortions are confined primarily to the local atomic environment around the dopants. Tables 1 and 2 present the bond lengths surrounding the impurity atoms for the rubidium- and cesium-doped systems, respectively, both prior to and following atomic relaxation. It is evident that the bond lengths between the dopant atoms and adjacent atoms increase after relaxation. This elongation can be attributed to the initial overlap and

repulsion of electron clouds before structural optimization. The most pronounced variation in bond length occurs between the impurities atoms and the neighboring nitrogen atoms, which is consistent with the relatively shorter distance between nitrogen and rubidium or cesium atoms compared to aluminum. Consequently, this elongation of the N–Rb and N–Cs bonds leads to a reduction in the Al–N bond lengths in both doped configurations.

Table 1: Bond lengths around the impurity atom for the rubidium-doped sample. Values are given in angstroms (Å).

Bond type	Rb-N	Rb-Al	Al-N
Before relaxation	1.7898	3.1000	1.7898
After relaxation	2.2778	3.2473	1.7300

Table 2: Bond lengths around the impurity atom for the cesium-doped sample. Values are expressed in angstroms (Å).

Bond type	Cs-N	Cs-Al	Al-N
Before relaxation	1.7898	3.1000	1.7898
After relaxation	2.2938	3.2578	1.7290

After relaxation, the electronic and magnetic properties were examined. Figures 7 and 8 show the density of states (DOS) plots for the monolayers doped with rubidium and cesium, respectively. Comparing these figures with the DOS of the pristine two-dimensional material (Figure 2) reveals that doping breaks the symmetry between the spin-up and spin-down states. Therefore, the magnetic moment is no longer zero, and calculations show that the magnetic moment is equal to ( $2m_B$ ). For the rubidium-doped monolayers, the Fermi level lies within the band gap, indicating that this material is a magnetic semiconductor. However, for the cesium-doped sample, the Fermi level for spin-up lies within the gap, while for spin-down it lies in the conduction band. Consequently, both materials, especially the cesium-doped two-dimensional material, are capable of producing fully spin-polarized currents, and thus can be utilized as spin filters for applications in spintronic devices.

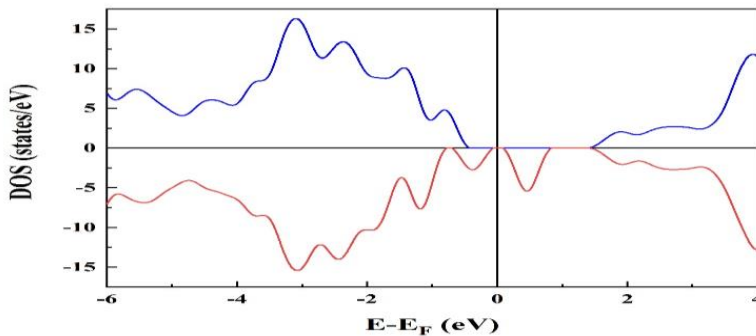


Figure 7: Density of states (DOS) plot of the AlN monolayer doped with rubidium. Using DFT calculations within the Quantum ESOERSSO simulation package.

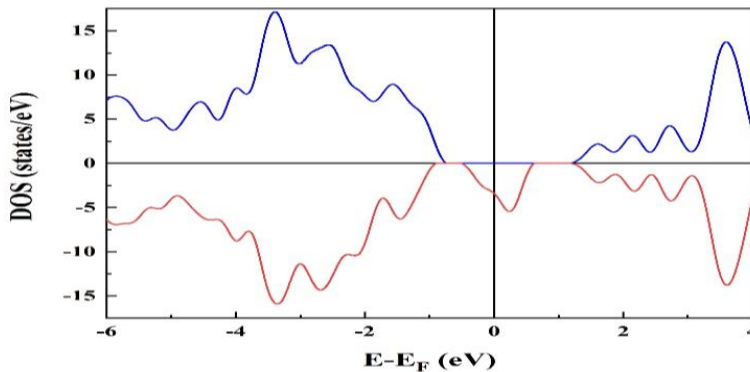


Figure 8: Density of states (DOS) plot of the AlN monolayer doped with Cesium. Using DFT calculations within the Quantum ESOERSSO simulation package.

Tables 3 and 4 respectively present the values of magnetic moment and electric charge of each atom in the compound. Considering the fact that the electronegativity of nitrogen is higher than that of the metallic elements, it appears that the electric charge has been transferred to the nitrogen atoms. Moreover, based on Table 4, the total magnetic moment mainly originates from the nitrogen atoms surrounding the impurity atom, and to some extent from the impurity atom itself. The magnetic moment of the aluminum atoms is negligible, and the magnetic coupling between aluminum atoms and other atoms is antiferromagnetic. The total magnetic moment of the cesium-doped compound is equal to  $2m_B$ , which is expected, since the magnetic moment of a half-metal must be an integer multiple of the Bohr magneton.

Table 3: The values of atomic electric charge in Rb- and Cs-doped samples.

Aluminum	Nitrogen	Impurity Atom	Compound Atom Type
1,8432	5,9802	8,0543	Doped with Rb
1,7490	5,7032	1,5611	Doped with Cs

Table 4: Magnetic moment values of atoms in Rb- and Cs-doped samples. The unit of the values is Bohr magneton( $\mu_B$ ).

Doping Type	Aluminum	Nitrogen	Impurity Atom	Total
Rb-doped	-0.0117	0.5699	0.1282	2
Cs-doped	-0.0111	0.5810	0.0850	2

#### 4. Conclusion

The origin of the magnetic moment is the presence of holes. Specifically, the impurity atom, which has one valence electron, substitutes an aluminum atom that has three valence electrons. In the pristine state, each nitrogen atom becomes an anion  $N^{-3}$  by accepting valence electrons from aluminum, meaning all its 2p orbitals are fully occupied and all spins are paired. Therefore, the three nearest aluminum neighbors collectively have 18 electrons. However, when an impurity atom replaces an aluminum atom, the three surrounding nitrogen atoms collectively have 16 electrons. This implies that doping introduces two holes in the nitrogen 2p orbitals, which leads to the emergence of  $2m_B$  magnetic moment.

As mentioned, the cesium-doped two-dimensional layer exhibits half-metallic behavior. According to the above discussion, it is observed that the largest contribution to the density of states at the Fermi level comes from the nitrogen 2p orbitals, with a smaller contribution from the aluminum 3p orbitals and the cesium 6p and 5d orbitals. In fact, the three narrow bands crossing the Fermi level in the band structure diagram for the spin-up states correspond to the three nitrogen 2p orbitals. This is consistent with the magnetic moment values shown in Table 4, where the majority of the magnetic moment originates from the nitrogen atoms. Based on this diagram, we conclude that the largest contribution to the magnetic moment of the compound specifically arises from the nitrogen 2p orbitals. The strong hybridization of the nitrogen p orbitals surrounding the impurity leads to p-p exchange interactions among the nitrogen atoms, which causes

a shift of the spin-up and spin-down states relative to each other. Consequently, the Fermi level lies within the gap for spin-up states and within the conduction band for spin-down states.

Spintronic devices have introduced new functionalities by utilizing magnetic materials and magnetic fields or the absence thereof in more stable memories, as well as in logic devices and magnetic sensors. Spintronic components operate based on a simple concept: first, information is stored as a specific spin orientation (up or down); then, these spins are coupled to moving electrons, and finally, the spin information is read out.

## 5. Reference

Bhatti, S., Sbiaa, R., Hirohata, A., Ohno, H., Fukami, S., & Piramanayagam, S. N. (2017). Spintronics based random access memory: a review. *Materials today*, 20(9), 530-548.

Bai, Y., Deng, K., & Kan, E. (2015). Electronic and magnetic properties of an AlN monolayer doped with first-row elements: a first-principles study. *RSC Advances*, 5(24), 18352-18358.

Chen, G. X., Wang, D. D., Wen, J. Q., Yang, A. P., & Zhang, J. M. (2016). Structural, electronic, and magnetic properties of 3d transition metal doped GaN nanosheet: A first-principles study. *International Journal of Quantum Chemistry*, 116(13), 1000–1005. <https://doi.org/10.1002/qua.25118>

Cui, Z., Wang, X., Li, E., Ding, Y., Sun, C., & Sun, M. (2018). Alkali-metal-adsorbed g-GaN monolayer: ultralow work functions and optical properties. *Nanoscale Research Letters*, 13. <https://doi.org/10.1186/s11671-018-2625-z>

Dean, C. R., Young, A. F., Meric, I., Lee, C., Wang, L., Sorgenfrei, S., ... & Hone, J. (2010). Boron nitride substrates for high-quality graphene electronics. *Nature nanotechnology*, 5(10), 722-726.

Fong, C. Y., Shaughnessy, M., Damewood, L., & Yang, L. H. (2012). Theory, experiment and computation of half metals for spintronics: recent progress in Si-based materials. *Nanoscale Systems: Mathematical Modeling, Theory and Applications*, 1, 1-22.

Ghasemzadeh, F., & Kanjouri, F. (2018). Strain effect on the electronic properties of III-nitride nanosheets: Ab-initio study. *Science China Technological Sciences*, 61(4), 535–541. <https://doi.org/10.1007/s11431-017-9177-1>

Gallagher, W. J., & Parkin, S. S. (2006). Development of the magnetic tunnel junction MRAM at IBM: From first junctions to a 16-Mb MRAM demonstrator chip. *IBM Journal of Research and Development*, 50(1), 5-23.

Han, R., Chen, X., & Yan, Y. (2017). Magnetic properties of AlN monolayer doped with group 1A or 2A nonmagnetic element: First-principles study. *Chinese Physics B*, 26(9). <https://doi.org/10.1088/1674-1056/26/9/097503>

Li, X., & Yang, J. (2016). First principles design of spintronics materials.

Paquin, F., Rivnay, J., Salleo, A., Stingelin, N., & Silva, C. (2015). Electrical Spin Injection and Transport in Semiconductor Nanowires: Challenges, Progress and Perspectives. *J. Mater. Chem. C*, 3, 10715–10722. <https://doi.org/10.1039/b000000x>

Wolf, S. A., Chtchelkanova, A. Y., & Treger, D. M. (2006). Spintronics—A retrospective and perspective. *IBM journal of research and development*, 50(1), 101-110.

Xia, J. B., Ge, W., & Chang, K. (2012). Semiconductor spintronics. World Scientific.

Zutic, I., Fabian, J., & Erwin, S. C. (2006). Bipolar spintronics: Fundamentals and applications. *IBM journal of research and development*, 50(1), 121-139.

Zutić, I., Fabian, J., & Sarma, S. D. (2004). Spintronics: Fundamentals and applications. *Reviews of modern physics*, 76(2), 323.

Zhang, Y., & Hou, Q. (2024). Alkaline earth metal-doped monolayer AlN: A DFT study of photocatalytic and magnetic properties. *Vacuum*, 228, 113520.